Bulletin of Engineering Geology and the Environment (2026) 85:181
https://doi.org/10.1007/s10064-026-04852-z

ORIGINAL PAPER

Fast landslide events in calcareous debris and weathered pyroclastic soils: a case study in Southern Italy

L. Massaro[1] · C. Cerrone[2,3,4] · M. De Falco[1,5] · E. Marino[1] · M. Pirone[1] · N. Santangelo[6] · A. Santo[1]

Received: 2 August 2025 / Accepted: 12 February 2026

Abstract
In this study, we analyse the occurrence of fast landslides developed in detrital limestone-dolomitic deposits and colluvium deposits on steep dolomitic slopes in Southern Italy. In the past few decades, the literature research on this type of landslide has mainly focussed on events developed in pyroclastic soils. However, the results of this study show that, even in weathered calcareous debris and with moderate deposit thickness (0.5–2 m), these phenomena can evolve into dangerous events. In the investigated area, the debris slides were mapped, providing a complete dataset of events that occurred in the 2022–2023 period. Successively, field and drone surveys enabled defining the stratigraphy of the involved deposits, the estimation of the mobilised volumes, and sampling for a preliminary lab-based geotechnical characterisation. Moreover, the rainfall data were acquired to identify their relationship with the landslide events. The results showed that the debris slides in the area involve cover deposits of moderate thickness (0.5–2 m) on slopes dipping from 27° to 45°. Most of the events developed a sliding surface at the interface between an ancient paleosoil and the detrital and colluvial deposits, mobilising downstream with significant runout and increasing volumes. Critical rainfall events, exceeding 100 mm daily, combined with antecedent periods of intense rainfalls, acted as key triggers for these landslides. This work provides valuable insights for land-use planning and risk mitigation strategies, particularly in the context of increasing rainfall due to global warming.

Keywords Fast landslide · Debris slide · Weathered pyroclastic soil · Calcareous debris · Landslide hazard

Introduction

Debris slides represent one of the most dangerous geological processes in mountainous areas, due to their capacity to progressively involve larger volumes and reach high velocity, as well as the abundance of potentially susceptible areas (Hungr et al. 2014). The main predisposing factors for this type of landslide are the presence of loose soil/colluvium of various thicknesses, covering steep slopes formed of a stronger substrate. The soil type, vegetation coverage, and land use play fundamental roles as preparatory factors. On the other hand, the triggering factors can be represented by heavy rainfall or seismic inputs (Sæmundsson et al. 2018; Yagi et al. 2009). The debris slide events are usually classified as an initial component of debris avalanches or debris flows, thus representing a mechanism of initiation for this kind of landslide (Hungr et al. 2014).

Studies on land management in mountainous areas rely on the analysis and forecast of the temporal and spatial distribution of instability phenomena, which should be specific

✉ C. Cerrone
ciro.cerrone@units.it; ciro.cerrone@unive.it

1 Department of Civil, Building and Environmental Engineering (DICEA), University of Naples Federico II, Naples, Italy

2 Department of Environmental Sciences, Informatics and Statistics (DAIS), University of Venice Ca' Foscari, Venice, Italy

3 Department of Mathematics, Informatics and Geosciences (MIGe), University of Trieste, Trieste, Italy

4 International Centre for Climate Change Research and Studies, Venice, Italy

5 Direzione del Genio Militare della Marina di Taranto, Ministry of Defence, Naples, Italy

6 Department of Earth, Environmental and Resources Sciences (DiSTAR), University of Naples Federico II, Naples, Italy

Published online: 05 March 2026

to an individual type of landslide. In this context, the data collection includes the total runout distance, sediment thickness, involved area, and mobilised volume, as well as information on past events in the area (Hungr 2005; Hürlimann et al. 2008; Sarkar et al. 2016). Therefore, the development of detailed and updated datasets on the landslide events is critical for the susceptibility management of an area. However, in some cases, the landslide morphological traces can be rapidly masked by the vegetation growth, weathering, or anthropogenic activity, making it more challenging to develop a debris slide inventory and susceptibility model in a specific area. In detail, the key parameters to be considered in a debris slide susceptibility analysis are the slope gradient and the loose sediment availability. The latter can vary within a wide range of thickness, with even 0.1 m thick deposits having a destructive potential by increasing their volume during the flow (Iverson 1997).

The understanding of debris slide phenomena has increased during the last decades, with several studies on their kinematics and hazard assessment. Overall, two types of approaches can be distinguished for the studies on the debris slide hazard susceptibility: (i) at the regional scale and (ii) at the local scale. The former applies large amounts of geo-spatial datasets to define, by means of numerical models, machine learning techniques, and statistical methods, the probability of landslide occurrence in the investigated area (Carrara et al. 2008; Dou et al. 2020; Guzzetti et al. 1999; Liu and Lei 2003; Meena et al., 2022). On the other hand, the local scale studies apply empirical methods based on fewer and site-specific parameters (Chau and Lo 2004; Crosta et al. 2003; Glade 2005; Pasuto and Soldati 2004).

In this study, we investigated the occurrence of numerous debris slide events that involved the colluvial and debris deposits lying on an ancient pyroclastic level, covering the dolostone slopes of a mountainous area between the Tyrrhenian side of Basilicata and Calabria regions (Southern Italy) The ancient pyroclastic level is intensely weathered, constituting a widely occurring paleosoil with 0.5–2 m thickness.

The study area, where low to moderate seismicity activities were recorded (Rovida et al. 2022), is comprised between the towns of Marina di Maratea (Basilicata Region) and Praia a Mare (Calabria Region), a coastal zone of great tourist and environmental importance. Moreover, the national routes *SS18* and *SS585* were affected at different points by the documented landslide events. The area has been repeatedly affected by Mediterranean Hurricanes (or Medicane) events, which triggered numerous landslides (Berardino et al. 2003; Castiglioni et al. 2024; Pellicani et al. 2016; Santo and Massaro 2024). Although Medicanes are smaller with respect to their tropical counterparts, this severe weather activity is frequent in the Mediterranean region and, in recent years, the scientific community's attention on the phenomena is growing due to their increasing destructive potential in land and coastal areas (Flaounas et al. 2022; Menna et al. 2023; Scardino et al. 2024).

The study is based on a multidisciplinary approach that integrates classical geomorphological and geotechnical analyses with modern remote-sensing techniques. The first step was to compile a geomorphological map of the area, after which the landslide events were mapped with ArcGIS Pro, providing a complete dataset of events that occurred in the 2022–2023 period. Successively, the recognized landslide events, that constitute the newly, generated dataset, were validated and implemented by means of field surveys. Such surveys (i) enabled the reconstruction of the stratigraphic setting of the area, (ii) the sampling of the deposits for a preliminary geotechnical characterisation of the involved deposits, (iii) the development of a detrital cover map of the area, and (iv) the photo acquisition of the damages caused to the buildings and road network. Moreover, drone flights permitted the development of the post-landslides DTM, which was used for the calculation of the mobilised volume of a major debris slide with the Dem of Difference (DoD) technique. The debris slide dataset was correlated with the rainfall data of the period to establish potential correlations between the precipitation and the triggering of the events. Also, the morphometric parameters were statistically analysed.

Although the investigated debris slide phenomena are very common in Italy and all around the world (Hungr et al. 2014), it is the first time that this kind of shallow debris slides occurring in a detrital cover of dolostone slopes are analysed in the study area, where rock landslides are predominant (Minervino et al. 2024; Santo and Massaro 2024). The collected data highlight the magnitude of debris slide events and the damage they produced. The main aim of this paper is to provide a robust multidisciplinary dataset that can improve the knowledge and serve as a valuable resource to be used in further hazard and risk assessment studies.

Methods and materials

The geological, geomorphological, and preliminary geotechnical characterisation of the landslide events of the investigated area was carried out with a multi-disciplinary workflow.

The first step consisted of the production of thematic maps of the examined area, based on the DTM elaborated with ArcGIS Pro from LiDAR data with a resolution of 1×1 m and 2×2 m released by the Italian Ministry of the Environment and Energy Security. The data gathering on the events that occurred in the 2022–2023 period was performed with ArcGIS Pro, digitising the landslide boundaries

of debris slide and alluvial events. The thematic maps and dataset were then validated and implemented with field and drone surveys. At the same time, the temporal information on the events was collected through an analysis of municipal reports, media, and bibliographic sources, defining two main events of landslide triggering: 13th October 2022, and 14th −15th June 2023.

The drone surveys were performed on major debris slides that were geologically more relevant or hazardous for the area. The drone used was a DJI™ Matrice 300 RTK quadrotor Unmanned Aerial Vehicle (UAV) platform equipped with a DJI™ P1 camera (full frame CMOS sensor, 45 MP resolution with 35 mm lens). Successively, the images were processed with Structure from Motion (SfM) computer vision techniques, developing a dense point cloud, from which the digital surface models (DSM), and different nadir, frontal and oblique orthomosaic images were elaborated. The developed digital elevation model (DEM) was compared with the pre-landslide DEM by computing the DoD with ArcGIS Pro, quantifying the mobilised volumes, and the areas of erosion and deposition within the landslide body.

Successively, the debris slide dataset was statistically analysed to investigate the morphometric parameters of the individual events. The parameters calculated include the area, crown and toe altitudes to define the vertical drop, horizontal length, total (crown-to-toe) length, slope angle of the sliding zone and crown area, angle of reach, distance from the road network, and mobilised volume.

The field surveys also enabled to (i) reconstruct the geological stratigraphic succession of the detrital cover (colluvial, debris, and paleosoil deposits) involved, (ii) sample the different levels for geotechnical laboratory tests, and (iii) perform the LiDAR surveys with drones. The definition of the stratigraphic succession characterising the study area, along with the construction of geological cross-sections that detail the varying thickness of the outcropping facies, facilitated the elaboration of the detrital cover map for the area.

Regarding the geotechnical characterisation, the soil specimens were sampled with cylindrical iron steel cutters, and grain size distributions, soil shear tests, and Atterberg limits were performed at the geotechnical laboratory of the Department of Civil, Building and Environmental Engineering (DICEA) of the University of Naples Federico II.

The rainfall data of the areawere collected from the rain gauge stations of Tortora (34 m above sea level, hereafter as a.s.l., 39° 56′ 11″ N, 15° 46′ 4″ E), Maratea Massa (533 m a.s.l., 39° 59’ 1” N, 15° 44’ 10” E), and Castrocucco (111 m a.s.l., 39° 59’ 32” N, 15° 48’ 7” E) for the three months preceding the individuated days when the debris slides were triggered, in October 2022, and June 2023. The rain gauge measurements are recorded every 10 min, from which we used the 24-h values and calculated the cumulative curves. Such a dataset enabled to investigate the potential correlation between rainfall and landslide events.

The impact of the landslide events was recorded with field surveys and photo acquisition in the days following the occurrence of the events. In some cases, the information was provided by the local authorities. The main villages affected were Castrocucco and Tortora, with damages to the infrastructure, buildings, beach resorts and the national roads *SS18 Tirrena Inferiore* and *SS585 Fondo Valle del Noce*.

Results

Geological and geomorphological analyses

The study area, which belongs to the fold-and-thrust-belt of the southern Apennines (Patacca et al. 1990), is characterised by a Meso-Cenozoic carbonates bedrock (Iannace et al. 2005; 2007, Fig. 1). The area was affected by the Quaternary extension (Rehault et al. 1987), with the opening of the Policastro Gulf and formation of coastal plains on the Tyrrhenian side of the chain (Santangelo et al. 2017). However, the coastal sector of the Policastro Gulf experienced uplift during the Quaternary as testified by raised marine terraces from a few metres a.s.l. up to 400 m a.s.l. along the Mt. Bulgheria (Ascione and Romano 1999; Cerrone et al. 2021a; De Santis et al. 2025; Esposito et al. 2003), and up to 240 m a.s.l. in northern Calabria (Carobene and Dai Pra 1990, 1991; Cerrone et al. 2021b; Filocamo et al. 2009).

A detailed geomorphological map of the investigated area has been provided (Fig. 1) along with the dataset of landslides. This highlighted the distribution and typology of landslides across the study area and enabled investigating the spatial and temporal characteristics of the slope instability events.

The geomorphological map (Fig. 1) integrates the main geomorphological elements characterising the area on the Mesozoic bedrock. Here, the Noce River alluvial plain enters the alluvial-coastal plain of Castrocucco before flowing into the Tyrrhenian Sea. Minor watercourses generate alluvial fans, which, sometimes, are terraced. A long pebbly beach between Castrocucco and Praia a Mare headlands limits the coastal plain. Structural slopes are made up of Mesozoic dolostones and subtend a transitional zone to the plain with raised marine terraces partially buried by terraced alluvial fans and colluvial footslope.

The dolostone slopes on which the instability phenomena developed are characterised by moderate relief energy, comprised between 200 m and 600 m, while the slope angles are frequently higher than 30°. Such a framework is determined by either tectonics, fluvial erosional (Noce River), or coastal erosional origins.

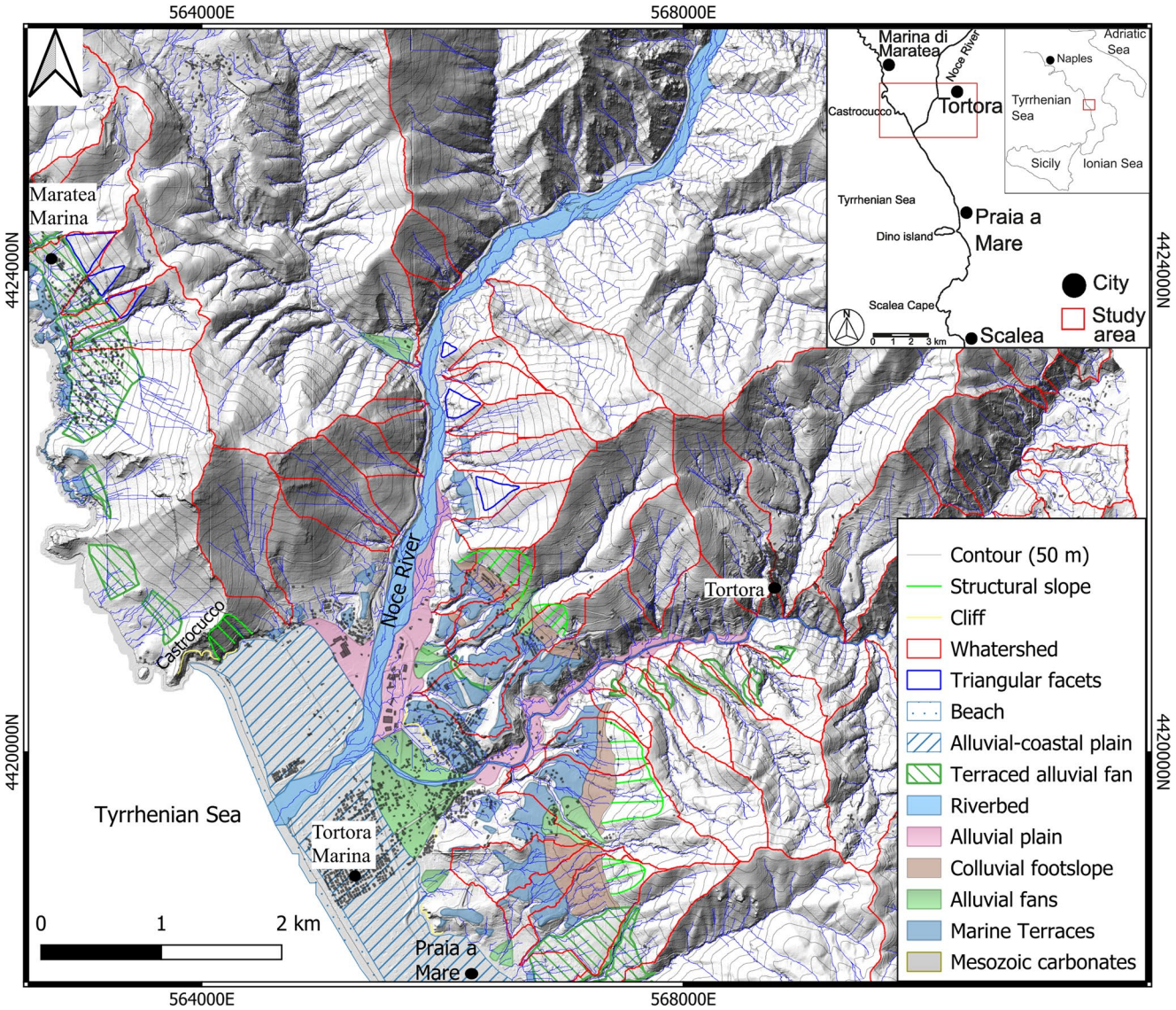

Fig. 1 Geological and geomorphological sketch of the study area

Stratigraphic succession

The field data collection on the sites of the major landslide events was aimed at (i) reconstructing the geological stratigraphic successions of the crown areas, (ii) determine the depth of the landslide body and the thickness of the layers involved, and (iii) collect samples for the geotechnical laboratory analyses (Sect. 3.2.4 below). The stratigraphic succession observed in the crown area (Fig. 2) can be considered as the most representative of the area and can be summarised as follows:

- the bedrock is represented by intensely fractured dolostones (dol) or, in some cases, ancient cemented breccias (br);
- above the bedrock, a highly weathered paleosoil (ps) of reddish colour is observed, with thickness varying in a 20 cm-1 m range, originating from the weathering and pedogenesis of older pyroclastic deposits. The level is massive and homogeneous, with no clast inclusions, and is results are generally dump, especially when collected at a few cm of depth;
- above the bedrock, a level of detrital and colluvial deposits (dcd) occurs, with about 2 m of thickness, characterised by dolomitic well-rounded clasts in a sandy calcareous-dolomitic matrix. It locally shows levels with a prevalence of finer (dcd_1) or coarser (dcd_2) clasts, defining an overall gravitative origin from the erosion processes of dolomitic slopes as either colluvial deposits or debris slides;

Fig. 2 Examples of crown areas used to reconstruct the stratigraphic succession, individuate the sliding surface, and sample the investigated levels (br: ancient cemented breccias, ps: paleosoil, dcd_1: finer detrital and colluvial deposits, dcd_2: coarser detrital and colluvial deposits, s: soil)

– on top of the succession, a soil level (s) of about 20–40 cm of thickness with a shrub-like vegetation is generally observed.

In most cases, the sliding surface was clearly observed at the interface between the red ancient paleosoil and the detrital and colluvial deposits (Fig. 3).

Maps of detrital cover and slope

The detrital cover thickness map (Fig. 4a) was created using high-resolution satellite images and validated with orthoimages, DTM of local landslide areas, and field surveys focussed on landslide crown areas (Fig. 2). The map is critical for the mountainous areas, where the landslide events are more likely to be triggered, excluding therefore the flat zones. The following three cover thickness classes were defined:

– 0–0.5 m: the dolomitic bedrock is outcropping or occasionally covered by 10–20 cm of paleosoil;
– 0.5–1 m: the cover deposits show thickness values between 0.5 cm and 1 m, forming a weathered red paleosoil on the dolomitic bedrock and, in turn, topped by the detrital and colluvial deposits;
– 1–2 m: the deposits thickness is higher than 1 m and, locally, higher than 2 m. In this case, the paleosoils are covered by 1–3 m of detrital and colluvial deposits.

The detrital cover map shows that, excepts for the watersheds and the crests, most of the slopes is characterised by not negligible cover thicknesses. The highest values (1–2 m class) are observed in the north-facing sectors, where for local climatic reasons the vegetation is more abundant and provides a limit to the erosion. Considerable thickness values also occur in the catchments, which are characterised by a wide presence of forest vegetation. The 0.5–1 m class is the most abundant in the area, favoured by the diffused occurrence of shrub-like vegetation rather than tall trees.

Furthermore, a map of the slope angle was developed from the LiDAR (Fig. 4b). The most represented class is the 27–35° in the mountainous areas, while steeper slopes

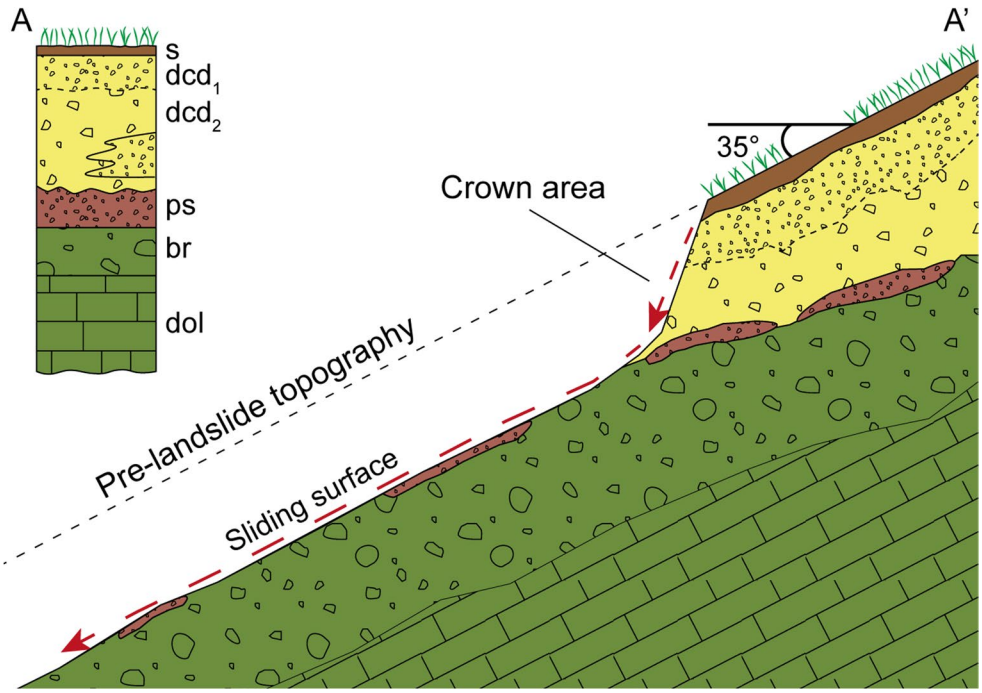

Fig. 3 Schematic cross-section of a debris slide crown area (A-A' trace in Fig. 2b) with the most representative stratigraphic column reconstructed for the examined area

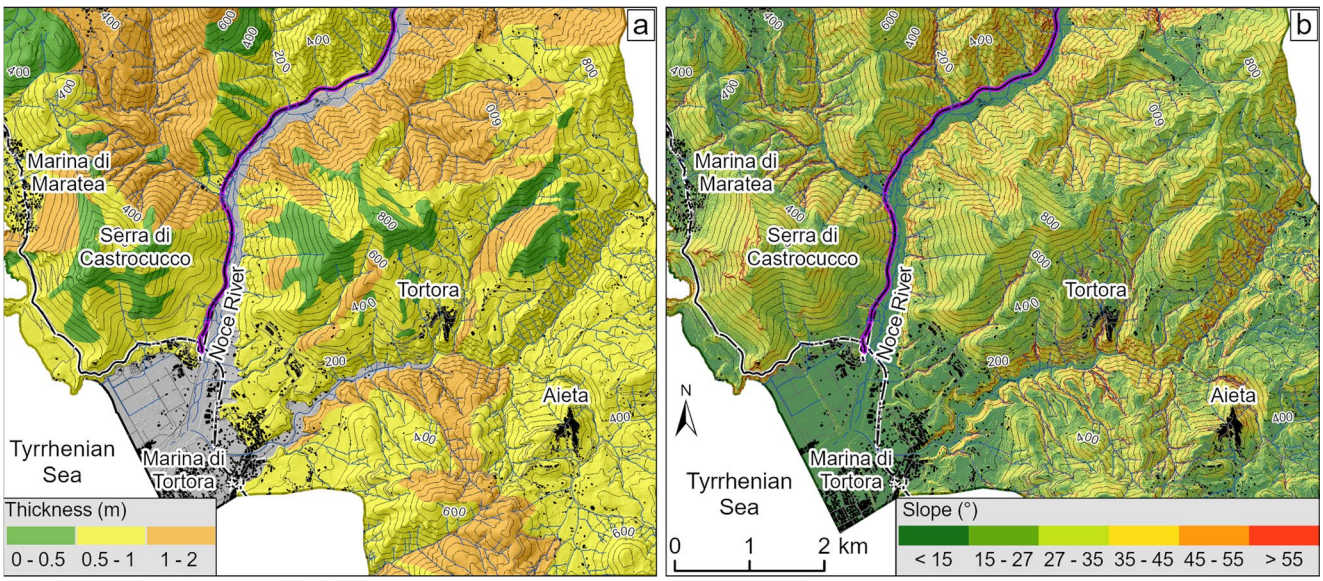

Fig. 4 (**a**) Detrital cover map showing the distribution of the three thickness classes (0–0.5 m, 0.5–1 m, 1–2 m) and (**b**) slope dip angles (°) of the examined area

(36–45°) occur in correspondence to geomorphological lineaments, along the water flows, or fault traces.

Landslide inventory map

The landslide inventory of the 2022–2023 events is shown in Fig. 5. The instability events were divided into debris slides and alluvial events, although the study and the successive analysis focus on the debris slides only. The latter were divided into channelled (18 events) and open-slope (unchanneled, 75 events) debris slides (Hungr et al. 2014). The spatial distribution of the landslides highlighted a higher concentration on the Noce River orographic left slopes, affecting the urban area of Tortora. Overall, the national road network has been affected by nine events (seven of which were debris slides), with remarkable impacts on the traffic viability.

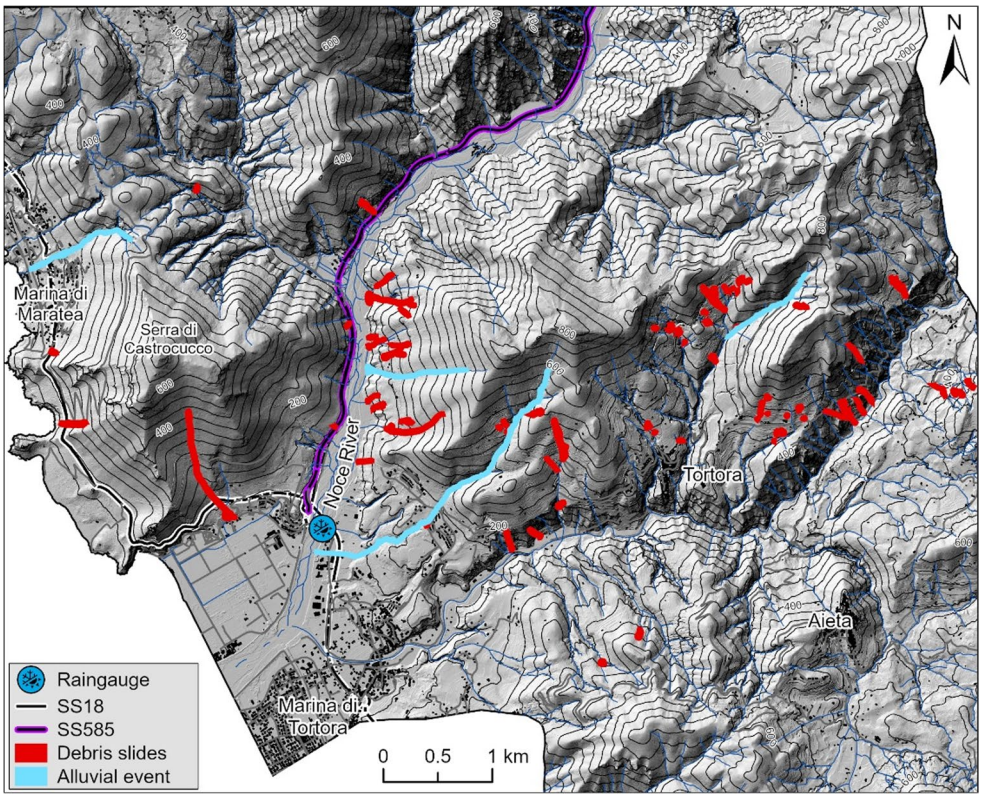

Fig. 5 Inventory map of the dataset collected on the instability events that occurred in the study area in the 2022–2023 period. The events were divided into debris slides (red) and alluvial events (light blue). The national roads SS18 and SS585 were highlighted to underline the impact of the landslides on the road network. The location of the Tortora rain gauge is shown (blue dot), while the others are beyond the map

In some cases, the satellite and drone-derived images enabled the observation of the debris slide evolution through time, as the example shown in Fig. 6. In this case, the interactions between landslide bodies developed at different times led to linking them together in a major slide that affected the underlying *SS18* national road. In detail, the

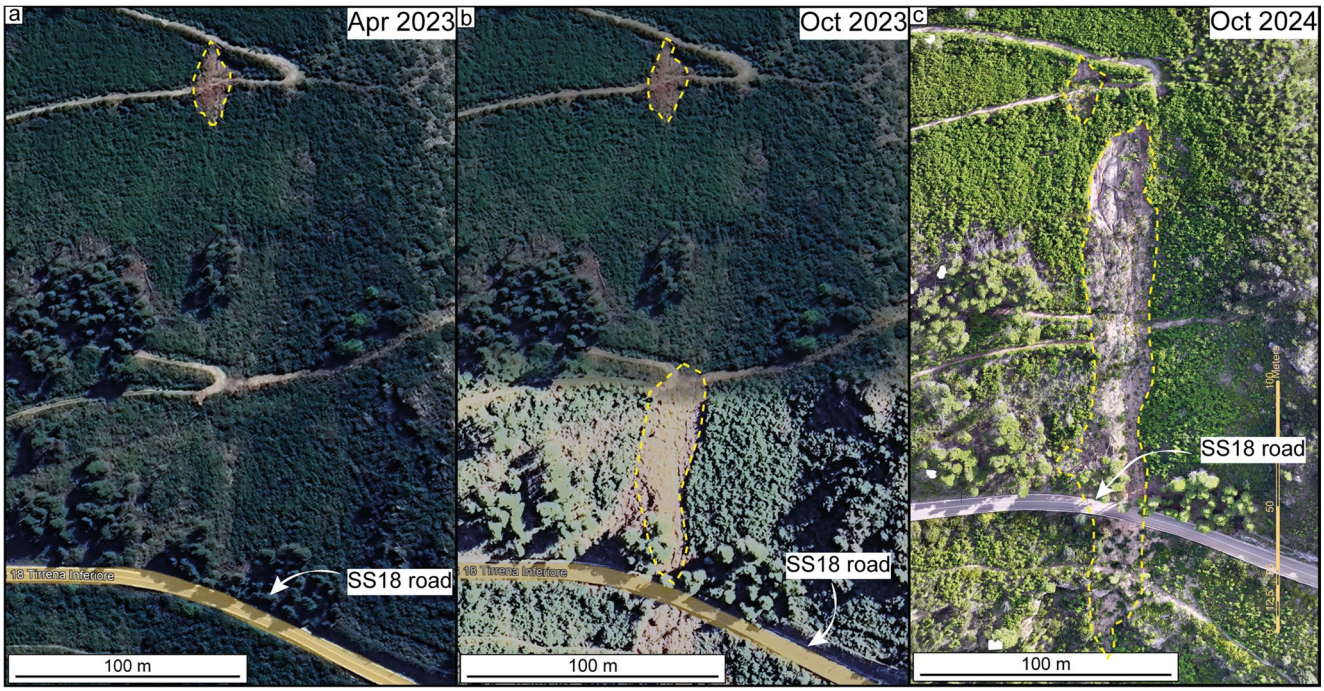

Fig. 6 Temporal evolution of a debris slide body (highlighted with the yellow dotted line) that affected the SS18 national road, observed by means of Google Earth images (**a**) 20th April 2023, and (**b**) 3rd October 2023) and drone-derived orthoimages (**c**) 28th October 2024)

landslide is activated firstly in the upper part (Fig. 6a) with a small scar developed in correspondence of a path trail. In Fig. 6b a different landslide took place in the lower part, with the crown developing in correspondence with another sector of the path trail, while the previous slide remained almost unaltered. The last image (Fig. 6c) shows the development of a third debris slide between the pre-existing ones, which connects to the lower slide and invades the *SS18* national road.

Morphometric analysis

The collected dataset on the landslide events characterising the study area was quantitatively analysed with ArcGIS Pro. The frequency distributions of some key physical characteristics of the debris slides were investigated, including slope angle (°), distance from the road (m), volume estimation (m^3), angle of reach (°), and the total (crown-to-toe) length of the landslide body (m). The alluvial events reported in Fig. 5 were not considered in this analysis, and the total dataset was composed of 93 debris slides.

The average slope dip and the crown dip angles were extrapolated from the DTM before the individual landslide events. Their frequency distributions (Fig. 7a) show that most of the debris slides (76%) developed on slopes dipping 27–45°, with 46% of the events comprised in the 27–35° range. Steep slopes are less ideal for this type of landslide, with only 3% of them occurring in slopes with dips > 45°. The crown dip angles are higher with respect to the overall slope, with an increase in the 36–45° interval. This may be favoured by local aspects, including anthropogenic works and variations of the bedrock morphology.

The angle of reach calculation was divided into two categories: channelled and open-slope debris slides. The dataset is mostly represented by open-slope debris slides rather than channelled, 75 and 18, respectively (Fig. 7b). The values obtained for the channelled events (78% comprised between 12 and 20°) are in line with what observed in high-velocity landslides in Southern Apennines (Revellino et al. 2004; Di Crescenzo and Santo 2005), while the open-slope events are characterised by higher angles (66% have angle of reach > 21°).

The volumes were estimated by using the thickness of the cover deposits (Fig. 7c) and the area of the individual crowns. The results show that the mobilised volumes vary in a wide range from a few tens to more than 10,000 m^3. However, more than half of the total dataset (56%) falls within the 500 m^3 range, while 35% of the debris slides have volumes comprised in the 501–2000 m^3 interval.

The length of the landslide bodies was calculated as the crown to toe distance and divided into the channelled (18 events) and open-slope (75 events) categories. The

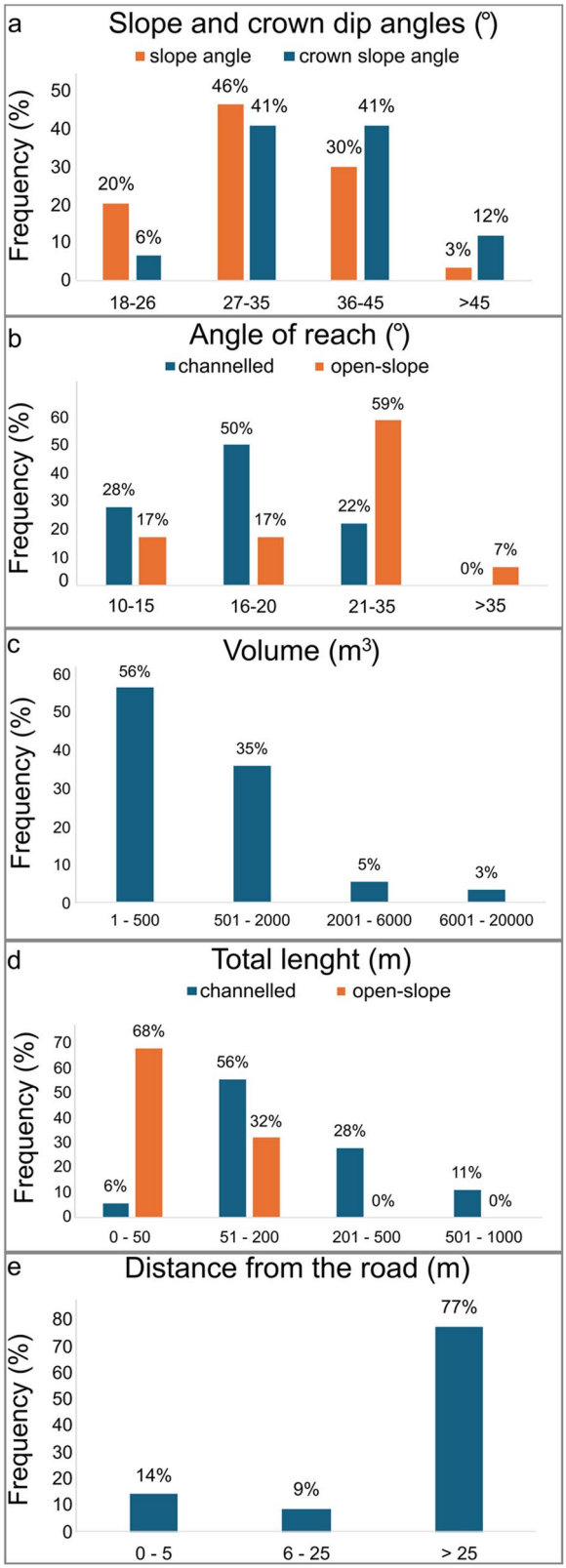

Fig. 7 Morphometric analysis of the digitised debris slide events showing the frequency distributions of (**a**) slope and crown dip angles (°), (**b**) angle of reach (°), (**c**) estimated volume (m^3), (**d**) total length of the landslide bodies (m), and (**e**) minimum distance from the road network (m)

frequency distribution (Fig. 7d) shows that in most cases (68%) the runout distance of the open-slope landslides is very limited (<50 m). However, 32% of them reached distances up to 200 m. As expected, the channelled debris slides show higher runout distances, with 39% of the dataset having a total length between 201 and 1000 m, and 56% falling into the 51–200 m interval.

The distance from the road was calculated as the minimum distance between the debris slide crown and the road network in order to evaluate the potential impact of the roads on the triggering of the landslides. The frequency distribution (Fig. 7e) shows that such a relationship did not occur, with 77% of the events taking place at more than 25 m from the roads. Therefore, it can be derived that most of the landslides were triggered by natural factors rather than anthropic influences.

Mobilised volumes

The volumes of the mobilised deposits during the individual debris slide events were quantitatively determined by means of the DoD computation. These were developed for the major events by using the drone-derived post-landslide DEM and the pre-landslide DEM obtained from LiDAR data released by the Italian Ministry of the Environment. In Fig. 8, an example of a DoD map for one of the major debris slides developed in the study area in the analysed period. The temporal evolution of these debris slides is illustrated in Fig. 6.

The DoD analysis shows that the crown area (790 m^2) of the major slide mobilised a volume of about 1500 m^3, with a total debris slide area of 3800 m^2. The smaller landslide (to the East), which developed before the larger one, mobilised a volume of about 100 m^3 for a total area of 350 m^2. In the major landslide, the erosion took place mainly in the crown area, with values up to 3.5 m of eroded deposits, and in some channels along the slope. The deposition areas correspond to the occurrence of terraces along the slope and the trail tracks, where the highest values of 2 m are observed. Moreover, most of the deposited material reached the *SS18* national road and was removed before the drone survey. Therefore, this represents an underestimation of the deposited volume involved in the analysed landslides.

Pluviometric data analysis

Two major events, occurring on 13 October 2022 and 14–15 June 2023, were examined. The daily rainfall, cumulative rainfall over the preceding three months, and hourly rainfall data were analysed from three different rain gauges, as summarised in Fig. 9. Such a rainfall dataset shows the significant role of both antecedent rainfalls and intense precipitation events in triggering the analysed landslides. The rainfall data, sourced from rain gauge stations in Maratea, Tortora, and Castrocucco, demonstrate consistent patterns of concentrated rainfall over short periods. These patterns align with the typical Mediterranean climatic regime, where autumnal and spring storms are characterised by brief but intense rainfall.

On 13 October 2022, most of the analysed landslides took place following rainfall events with daily values of 150–160 mm and hourly peaks of up to 50 mm. The cumulative curves of the three months preceding the events show a similar pattern from all the rain gauge stations, reaching values of 450–500 mm and recording higher rainfalls during the September-October period. The hourly data of the

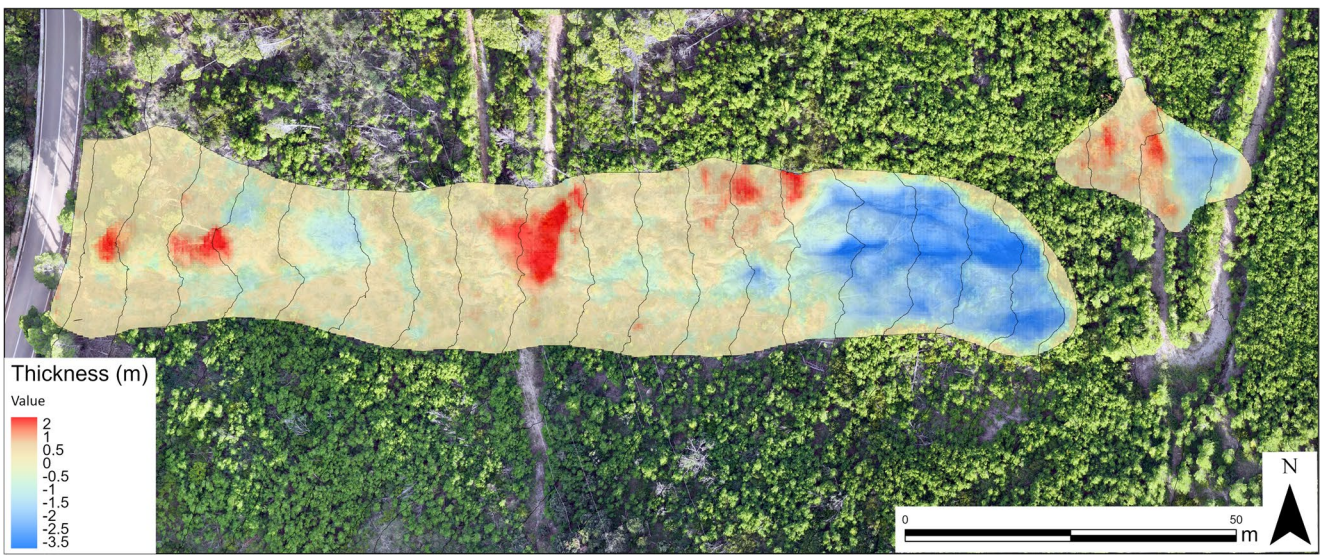

Fig. 8 Example of DoD map computed for major landslides developed in the 2022–2023 period

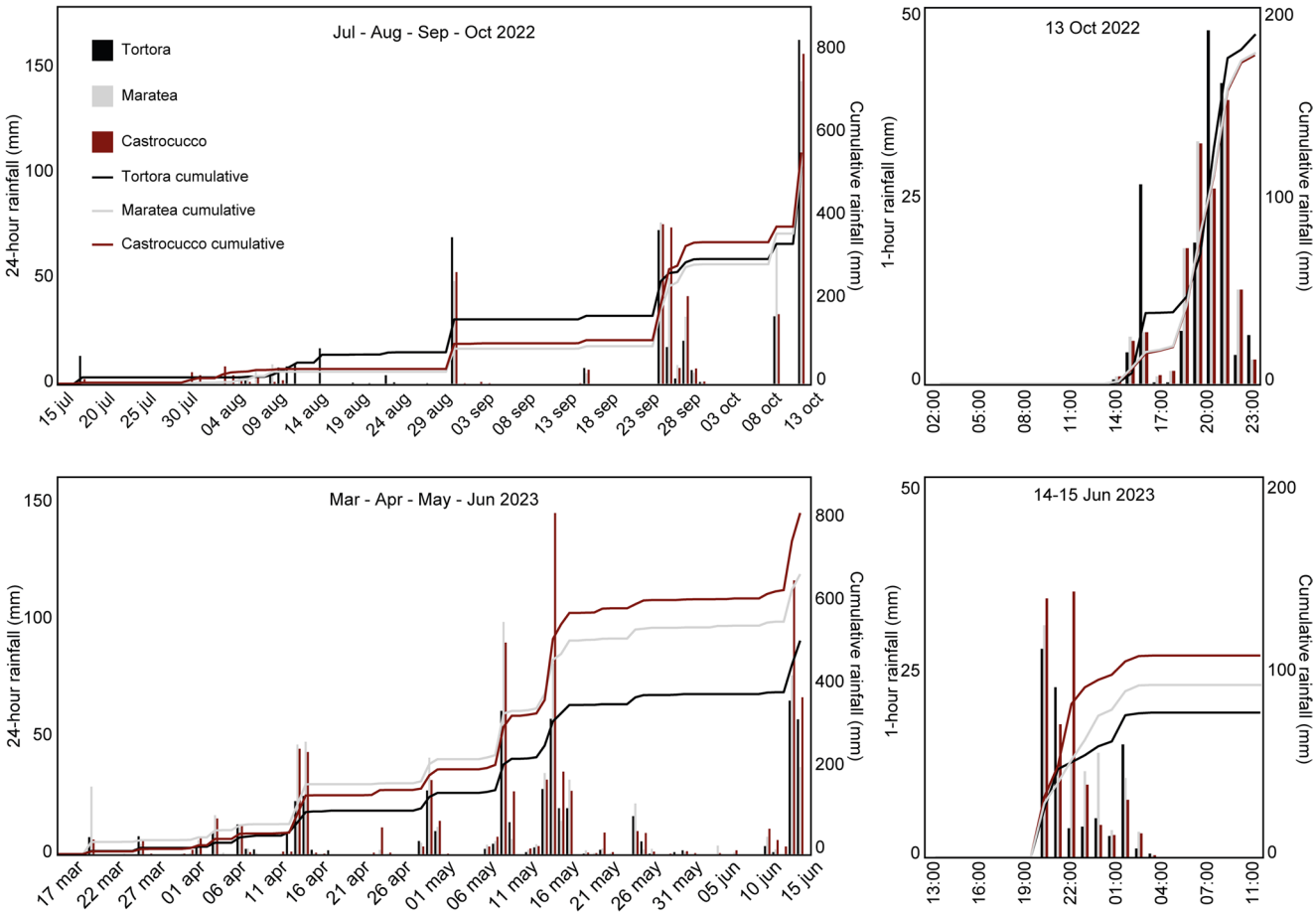

Fig. 9 Rainfall data collected from the three rain gauge stations of Tortora, Maratea Massa, and Castrocucco, for the three months preceding the landslide events. The 24-hour rainfall with cumulative curves is shown for the three months preceding the events, while the 1-hour rainfall with cumulative curves is shown for the day of the events

day of the events show that different trends are displayed by the rain gauge stations, with Maratea rain gauge having one main peak (about 35 mm), while Tortora recorded three distinct peaks (28 mm, 49.6 mm, and 42.2 mm), and Castrocucco shows 34 mm and 39.8 mm peaks. The spatial variability of the hourly events and the distinct peaks recorded in the different rain gauge stations in coastal and inland areas recording, suggest storm movements inland.

The 14–15 June 2023 event exhibited daily totals of up to 117 mm (Castrocucco), while the three months cumulative curves show different recorded values, with the highest (795 mm) at Castrocucco and the lowest (610 mm) at Tortora rain gauges. The highest hourly intensity was recorded in one clear peak at Maratea (27 mm), two at Tortora (25 and 20 mm), and two at Castrocucco (30 and 32 mm).

Geotechnical characterisation

Grain size distribution curves were obtained for seven samples collected in the field, four from the *ps* layer and three from the *dcd* layer (Fig. 10). The samples taken from the uppermost layer (*dcd*) indicate a relatively narrow envelope for a highly heterogeneous material composed of gravel with sand and silt. In contrast, the samples from the *ps* layer contain a higher percentage of fine-grained soil compared to the surface layer and define an envelope that encompasses soils ranging from sand with clayey silt to sand with silt and clay. For the *ps* layer samples, Atterberg limits were determined on the fine fraction. Specifically, the liquid limit (w_L) averaged 70%, while the plasticity index (I_p) was 38%, values corresponding to an inorganic clay of medium to high plasticity.

For determining the mechanical characterisation of the layer where the slip surface is typically located, direct shear tests with submersion during consolidation were conducted on specimens sampled from the *ps* layer. The shear phase was carried out at a rate of 0.005 mm/min.

Only four tests could be performed at normal stress levels of 20, 30, 40, and 80 kPa, due to both the difficulty in collecting undisturbed samples — given the presence of

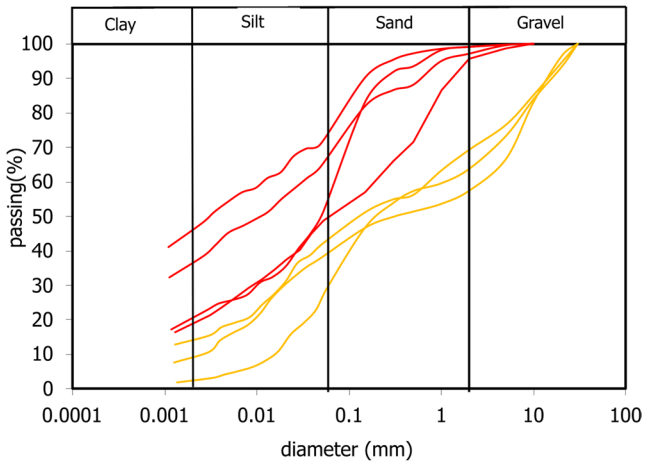

Fig. 10 Grain size distributions of samples collected from lithotype dcd (n°=3) and ps (n°=4)

coarse material accounting for 20% to 40% by weight — and operational challenges related to the presence of inclusions, which compromised the success of several tests. As a result, the mechanical characterization is considered preliminary, and the critical state envelope is presented in Fig. 11, along with the physical properties of the specimens (ID 1–4) measured at the beginning of the test. The initial value of the porosity (n) is approximately 0.46 on average, while that of dry unit weight, γ_d, is about 14.2 kN/m³. Additionally, the specimens were found to be in a partially saturated state. Notably, the specimen tested under a vertical stress of 20 kPa differs from the other three specimens in terms of porosity and initial degree of saturation, exhibiting a porosity 20% higher than the least porous specimen and a degree of saturation 18% lower than the most saturated specimen. Nevertheless, all specimens were saturated during the consolidation phase.

At the investigated stress levels, the envelope appears curvilinear, as typically expected for coarse-grained soils. The data were interpreted using polynomial regression, whose equation proved effective for the range of normal stress levels investigated, and is shown in Fig. 11a. However, assuming a linear Mohr–Coulomb envelope (conservative for that normal stress level) obtained through linear regression (black line in Fig. 11), the friction angle is approximately 33°.

Even if the data for the specimen tested at 20 kPa vertical stress are disregarded, the polynomial envelope remains unchanged, while the linear strength envelope yields a friction angle approximately 0.5° lower.When modelling the slopes affected by rapid landslides as infinite slopes and considering that the average slope angle in the initiation area is around 35°, a friction angle of approximately 33° supports a triggering mechanism driven by the complete saturation of the superficial *dcd* layer. Additionally, the significantly finer grain size of the *ps* layer compared to the *dcd* layer could create a permeability contrast between the two, promoting the formation of a perched water table within the *ps* layer. This, in turn, could lead to the development of positive pore water pressures, ultimately triggering rapid flowslides. However, these considerations are preliminary, and further geotechnical investigations are required to gain a deeper understanding of the hydromechanical behaviour of the cover material.

Damage report

The numerous debris slide events triggered in the analysed 2022–2023 period occurred in a rural area but affected the road network in several sectors, causing problems to the traffic viability. In particular, the national roads *SS585* and *SS18* were invaded by the mobilised deposits in at least nine points (seven debris slides and two alluvial events), causing the road closure and luckily with no people harmed. These two national roads represent critical

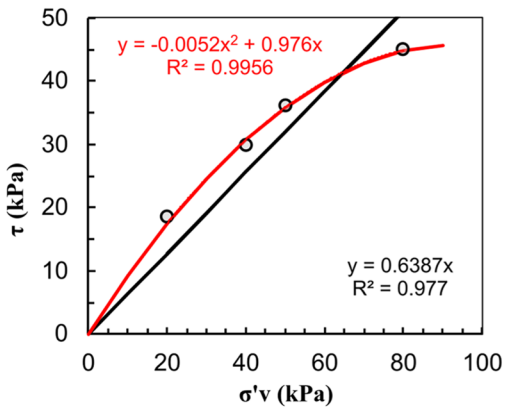

ID.	σ'v (kPa)	γd (KN/m³)	wn (%)	γ (KN/m³)	n -	Sr (%)
20	20	12.3	31	16.5	0.54	0.70
40	40	15.2	23	18.7	0.42	0.82
50	50	14.1	29	18.1	0.47	0.86
80	80	15.1	24	18.8	0.43	0.85

Fig. 11 Failure envelope at critical state with initial physical properties of the soil specimens subjected to test. The black line is the linear envelope; the red line is the non-linear envelope

Fig. 12 Photo collection of damages at the urban area and infrastructure of the October 2022 event, with the landslide affecting (**a**) the national road SS585, (**b**) the urban area of Castrocucco, (**c**) the national railway network in Marina di Maratea, and (**d**) a secondary road

viability branches between the Calabria and Basilicata regions since a national motorway is not present in the area. The regularity of the traffic viability is fundamental, especially in summer, with impacts on the tourism, which represents the main economy of the area. In Fig. 12, some examples of the documented landslide events and damages to the infrastructure and road network are shown. In other cases, the debris slides developed for remarkable run out distances, reaching the urban areas, such as in Castrocucco village, where a debris slide event involved several houses and infrastructure on the 13th October 2022 (Fig. 12b). Figure 12c-d document events affecting the critical railway network that connects Southern and Northern Italy, and a secondary road, respectively.

Discussion

Debris slides can cause significant damage to both property and human life, primarily due to the unpredictability, high velocity, and impact energy they generate. These events are common worldwide (Sidle and Swanston 1982; Wang et al. 2003; Jaiswal et al. 2011) and, more locally, in Southern Italy, where numerous studies have focused on debris slides occurring in pyroclastic deposits in the Campania region (Revellino et al. 2004; Di Crescenzo and Santo 2005). This research has been particularly relevant following the tragic Sarno event of 1988 (Crosta and Dal Negro 2003), which highlighted the destructive potential of such landslides even in areas with moderate

pyroclastic cover (Revellino et al. 2004; Di Crescenzo and Santo 2005; Guadagno et al. 2005; De Falco et al. 2023). Other studies investigated the occurrence of debris slides in the weathered layers of igneous-metamorphic massifs in Calabria and Sicily (Aronica et al. 2012; Del Ventisette et al. 2012). However, to date, no studies have documented debris slides similar to those occurring between Basilicata and Calabria regions, which involve detrital limestone-dolomitic deposits and colluvium lying on late Quaternary altered and clay-rich paleosoils, situated on steep dolomitic slopes. Even so, the role of soils and their relationship with rainfall accumulation have been widely investigated, although not always in relation to detrital–colluvial covers composed of detrital limestone-dolomitic deposits and colluvium deposits (e.g., Hollingsworth and Kovacs 1981; Qing-zhao et al. 2019; Tung et al. 2021; Ebrahim et al. 2025).

The debris slides in the study area involve cover deposits of limited thickness (0.5–2 m) lying on steep limestone-dolomitic slopes, with the highest frequency of events triggered in areas with slopes dipping from 27° to 45° (Fig. 7).

The paleosoil (ps), in which the sliding surfaces develop, consists of sand with silt and clay, with a higher proportion of fines compared to the overlying detrital layer. The presence of sand, however, gives it a relatively high critical friction angle of 33°, which, together with the increased resistance due to the partial saturation state, explains the stability of the cover materials on slopes less than 30°. The triggering of landslides occurs, instead, on slopes greater than 27–35°, as confirmed by the landslide inventory data (Fig. 7a), and during intense rainfall events capable of fully saturating the cover deposits.

Most of the investigated landslides developed a sliding surface at the interface between the ancient paleosoil (ps), finer and typically exhibiting low permeability, and the coarser detrital and colluvial deposits (dcd) on top of them (Fig. 3). The latter (dcd) are approximately two meters thick and in a state of partial saturation. These deposits mobilise on the slopes, exhibiting fluidisation effects and amplification downstream, with runout and volumes that can sometimes reach considerable values (thousands of cubic meters), especially when compared to the relatively modest slope energies where the landslides were triggered.

The laboratory analyses performed on the *dcd* and *ps* samples represented only a preliminary geotechnical characterisation of such levels. The main limitations were determined by the restricted number of samples. This issue was mainly addressed to the abundant presence of coarse material, occurrence of inclusions, and irregularity of the layers. Such aspects should be further investigated in future studies. However, the obtained friction angle value could be used in future studies aimed at developing susceptibility maps in the region or in similar contexts.

From the analysis of critical rainfall events, it is worth noting that in both cases in Maratea the critical daily rainfall exceeded 100 mm, a typical threshold for triggering debris flows in pyroclastic covers resting on limestone massifs in the Campania region (Guglielmi et al. 2023; Pirone et al., 2023; 2025). The antecedent rainfall over the three months period preceding the critical event, which acts as a preparatory factor for such phenomena (Santo et al. 2018; Pirone et al., 2023), exceeded 450 mm, aligning with values observed for similar events in the geological context of the Lattari Mountains (Forte et al. 2019).

Conclusions

In this study, the occurrence of fast landslides developed in detrital limestone-dolomitic deposits and colluvium deposits on steep dolomitic slopes was investigated. The recent literature research on this type of landslide has mainly focussed on events developed in pyroclastic soils. The multidisciplinary analyses conducted in this study and the associated dataset highlighted how, even in weathered calcareous debris and with moderate deposit thickness (0.5–2 m), these phenomena can evolve into dangerous events. Furthermore, the study provides valuable information for the future development of susceptibility maps for the northern Tyrrhenian Calabria-Basilicata (Southern Italy) calcareous slopes. The collected inventory revealed that large portions of the area are susceptible to landslides, with a potential involvement of significant road infrastructures downstream, thus presenting remarkable risk and high social impact. The integration of field surveys, aerial photo interpretations, and GIS-based analyses allowed for the creation of a reliable and high-resolution inventory, facilitating further studies on landscape dynamics and risk mitigation strategies. Moreover, the collected landslide data showed that, in most cases, the sliding surfaces developed at the interface between the ancient paleosoil and the detrital and colluvial deposits. The former, having a finer composition, typically exhibits low permeability in contrast with the more permeable and partially saturated *dcd* layer above it. This creates the conditions for the development of positive water pressures acting as a potential trigger to rapid flowslides.

These new data thus define the occurrence of potentially hazardous landslide events even for slopes with widespread detrital covers of gravelly-sandy and limestone nature, expanding the potential areas at risk. This is especially important considering the increasing frequency of intense daily rainfall events in recent years, which can be linked to

global warming. This work represents a preliminary investigation into the triggering mechanisms of debris slides involving detrital covers on carbonate massifs of the Southern Apennines, and it could be useful for more in-depth analyses aimed at defining susceptibility and risk from debris slides, particularly for agencies involved in land-use planning.

Acknowledgements Our thanks go to the editor and two anonymous reviewers, whose constructive feedback significantly contributed to improving the manuscript.

Funding Open access funding provided by Università degli Studi di Trieste within the CRUI-CARE Agreement. The work included in this study benefited from the support of DPC ReLUIS 2024–2026 (Scientific Coordinator Prof Antonio Santo) project, WP16, funded by the University of Naples, and from the financial support of the Agreement DICEA-Commissario di Governo Comune di Maratea (Scientific Responsible Prof Antonio Santo). Open access for this publication was facilitated by the support of the University of Trieste under the Springer–CRUI CARE agreement.

Declarations

Competing interests The authors have no relevant financial or non-financial interests to disclose.

References

Aronica GT, Brigandí G, Morey N (2012) Flash floods and debris flow in the city area of Messina, north-east part of Sicily, Italy in October 2009: the case of the Giampilieri catchment. Nat Hazards Earth Syst Sci 12:1295–1309. https://doi.org/10.5194/nhess-12-1295-2012

Ascione A, Romano P (1999) Vertical movements on the eastern margin of the Tyrrhenian extensional basin. New data from Mt. Bulgheria (Southern Apennines, Italy). Tectonophysics 315:337–356. https://doi.org/10.1016/S0040-1951(99)00279-6

Berardino P, Costantini M, Franceschetti G et al (2003) Use of differential SAR interferometry in monitoring and modelling large slope instability at Maratea (Basilicata, Italy). Eng Geol 68:31–51. https://doi.org/10.1016/S0013-7952(02)00197-7

Carobene L, Dai Pra G (1990) Genesis, chronology and tectonics of the Quaternary marine terraces of the Tyrrhenian coast of northern Calabria (Italy). Their correlation with climatic variations. Il Quaternario – Alp Mediterranean Quaternary 3(2):75–94

Carobene L, Dai Pra G (1991) Middle and Upper Pleistocene sea level highstands along the Tyrrhenian coast of Basilicata (Southern Italy). Il Quaternario – Alp Mediterranean Quaternary 4(1a):173–202

Carrara A, Crosta G, Frattini P (2008) Comparing models of debris-flow susceptibility in the alpine environment. Geomorphology 94:353–378. https://doi.org/10.1016/j.geomorph.2006.10.033

Castiglioni M, Caraffa T, Ottavi C et al (2024) Rockfall early warning system for enhancing traffic safety. New Challenges in Rock Mechanics and Rock Engineering - Proceedings of the ISRM Rock Mechanics Symposium, EUROCK 2024, CRC Press, pp 1459–1464

Cerrone C, Vacchi M, Fontana A, Rovere A (2021a) Last Interglacial sea-level proxies in the western Mediterranean. Earth Syst Sci Data 13:4485–4527. https://doi.org/10.5194/essd-13-4485-2021

Cerrone C, Ascione A, Robustelli G et al (2021b) Late Quaternary uplift and sea level fluctuations along the Tyrrhenian margin of Basilicata - northern Calabria (southern Italy): New constraints from raised paleoshorelines. Geomorphology 395:107978. https://doi.org/10.1016/j.geomorph.2021.107978

Chau KT, Lo KH (2004) Hazard assessment of debris flows for Leung King Estateof Hong Kong by incorporating GIS with numerical-simulations. Nat Hazards Earth Syst Sci 4:103–116. https://doi.org/10.5194/nhess-4-103-2004

Crosta GB, Dal Negro P (2003) Observations and modelling of soil slip-debris flow initiation processes in pyroclastic deposits: the Sarno 1998 event. Nat Hazards Earth Syst Sci 3:53–69. https://doi.org/10.5194/nhess-3-53-2003

Crosta GB, Dal Negro P, Frattini P (2003) Soil slips and debris flows on terraced slopes. Nat Hazards Earth Syst Sci 3:31–42. https://doi.org/10.5194/nhess-3-31-2003

De Falco M, Forte G, Marino E et al (2023) UAV and field survey observations on the November 26th 2022 Celario flowslide, Ischia Island (Southern Italy). J Maps 19:2261484. https://doi.org/10.1080/17445647.2023.2261484

De Santis V, Cerrone C, Meschis M, Scicchitano G, Ascione A, Caldara M (2025) Reoccupation of late Quaternary relative sea level indicators in a tectonically quasi-stable coastal area in Southern Italy (Cilento headland): insights into the Last Interglacial stillstands. Geomorphology 478:109692. https://doi.org/10.1016/j.geomorph.2025.109692

Del Ventisette C, Garfagnoli F, Ciampalini A et al (2012) An integrated approach to the study of catastrophic debris-flows: geological hazard and human influence. Nat Hazards Earth Syst Sci 12:2907–2922. https://doi.org/10.5194/nhess-12-2907-2012

Di Crescenzo G, Santo A (2005) Debris slides–rapid earth flows in the carbonate massifs of the Campania region (Southern Italy): morphological and morphometric data for evaluating triggering susceptibility. Geomorphology 66:255–276. https://doi.org/10.1016/j.geomorph.2004.09.015

Dou J, Yunus AP, Bui DT et al (2020) Improved landslide assessment using support vector machine with bagging, boosting, and stacking ensemble machine learning framework in a mountainous watershed. Japan Landslides 17:641–658. https://doi.org/10.1007/s10346-019-01286-5

Ebrahim K, Abdelkader EM, Zayed T, Meguid MA (2025) A deep learning-based model for endorsing predictive accuracies of landslide prediction: insights into soil moisture dynamics. Geoenvironmental Disasters 12:36. https://doi.org/10.1186/s40677-025-00333-9

Esposito C, Filocamo F, Marciano R et al (2003) Late Quaternary shorelines in southern Cilento (Mt. Bulgheria): morphostratigraphy and chronology. Il Quaternario – Alp Mediterranean Quaternary 16(1):3–14. https://amq.aiqua.it/index.php/amq/article/view/587

Filocamo F, Romano P, Di Donato V et al (2009) Geomorphology and tectonics of uplifted coasts: New chronostratigraphical constraints for the Quaternary evolution of Tyrrhenian North Calabria (southern Italy). Geomorphology 105:334–354. https://doi.org/10.1016/j.geomorph.2008.10.011

Flaounas E, Davolio S, Raveh-Rubin S et al (2022) Mediterranean cyclones: current knowledge and open questions on dynamics, prediction, climatology and impacts. Weather Clim Dynamics 3:173–208. https://doi.org/10.5194/wcd-3-173-2022

Forte G, Pirone M, Santo A et al (2019) Triggering and predisposing factors for flow-like landslides in pyroclastic soils: the case study of the Lattari Mts. (southern Italy). Eng Geol 257:105137. https://doi.org/10.1016/j.enggeo.2019.05.014

Glade T (2005) Linking debris-flow hazard assessments with geomorphology. Geomorphology 66:189–213. https://doi.org/10.1016/j.geomorph.2004.09.023

Guadagno FM, Forte R, Revellino P et al (2005) Some aspects of the initiation of debris avalanches in the Campania Region: the role of morphological slope discontinuities and the development of failure. Geomorphology 66:237–254. https://doi.org/10.1016/j.geomorph.2004.09.024

Guglielmi S, Pirone M, Dias AS, Cotecchia F, Urciuoli G (2023) Thermohydraulic Numerical Modeling of Slope-Vegetation-Atmosphere Interaction: Case Study of the Pyroclastic Slope Cover at Monte Faito, Italy. J Geotech GeoEnviron Eng 149. https://doi.org/10.1061/JGGEFK.GTENG-11240

Guzzetti F, Carrara A, Cardinali M, Reichenbach P (1999) Landslide hazard evaluation: a review of current techniques and their application in a multi-scale study. Cent Italy Geomorphology 31:181–216. https://doi.org/10.1016/S0169-555X(99)00078-1

Hollingsworth R, Kovacs GS (1981) Soil Slumps and Debris Flows: Prediction and Protection. EnvironmentalEngineering Geoscience xviii:17–28. https://doi.org/10.2113/gseegeosci.xviii.1.17

Hungr O (2005) Classification and terminology. In: Jakob M, Hungr O (eds) Debris-flow hazards and related phenomena. Springer Berlin Heidelberg, Praxis, pp 9–23

Hungr O, Leroueil S, Picarelli L (2014) The varnes classification of landslide types, an update. Landslides 11:167–194. https://doi.org/10.1007/s10346-013-0436-y

Hürlimann M, Rickenmann D, Medina V, Bateman A (2008) Evaluation of approaches to calculate debris-flow parameters for hazard assessment. Eng Geol 102:152–163. https://doi.org/10.1016/j.enggeo.2008.03.012

Iannace A, Bonardi G, D'Errico M et al (2005) Structural setting and tectonic evolution of the Apennine Units of northern Calabria. Comptes Rendus - Geoscience 337:1541–1550. https://doi.org/10.1016/j.crte.2005.09.003

Iannace A, Vitale S, D'Errico M et al (2007) The carbonate tectonic units of northern Calabria (Italy): a record of Apulian palaeomargin evolution and Miocene convergence, continental crust subduction, and exhumation of HP-LT rocks. J Geol Soc Lond 164:1165–1186

Iverson RM (1997) The physics of debris flows. Rev Geophys 35:245–296. https://doi.org/10.1029/97RG00426

Jaiswal P, van Westen CJ, Jetten V (2011) Quantitative estimation of landslide risk from rapid debris slides on natural slopes in the Nilgiri hills, India. Nat Hazards Earth Syst Sci 11:1723–1743. https://doi.org/10.5194/nhess-11-1723-2011

Liu X, Lei J (2003) A method for assessing regional debris flow risk: an application in Zhaotong of Yunnan province (SW China). Geomorphology 52:181–191. https://doi.org/10.1016/S0169-555X(02)00242-8

Meena SR, Soares LP, Grohmann CH et al (2022) Landslide detection in the Himalayas using machine learning algorithms and U-Net. Landslides 19:1209–1229. https://doi.org/10.1007/s10346-022-01861-3

Menna M, Martellucci R, Reale M et al (2023) A case study of impacts of an extreme weather system on the Mediterranean Sea circulation features: Medicane Apollo (2021). Sci Rep 13:3870. https://doi.org/10.1038/s41598-023-29942-w

Minervino Amodio A, Corrado G, Gallo IG et al (2024) Three-Dimensional Rockslide Analysis Using Unmanned Aerial Vehicle and LiDAR: The Castrocucco Case Study, Southern Italy. Remote Sens (Basel) 16:2235. https://doi.org/10.3390/rs16122235

Pasuto A, Soldati M (2004) An integrated approach for hazard assessment and mitigation of debris flows in the Italian Dolomites. Geomorphology 61:59–70. https://doi.org/10.1016/j.geomorph.2003.11.006

Patacca E, Sartori R, Scandone P (1990) Tyrrhenian basin and Apenninic Arcs: kinematic relations since Late Tortonian times. Mem Soc Geol It 45:425–451. https://doi.org/10.1007/978-94-011-2016-6_7

Pellicani R, Spilotro G, Van Westen CJ (2016) Rockfall trajectory modeling combined with heuristic analysis for assessing the rockfall hazard along the Maratea SS18 coastal road (Basilicata, Southern Italy). Landslides 13:985–1003. https://doi.org/10.1007/s10346-015-0665-3

Pirone M, Di Maio R, Forte G et al (2023) Study of the groundwater regime in unsaturated slopes prone to landslides by multidisciplinary investigations: Experimental study and numerical modelling. Eng Geol 315:107045. https://doi.org/10.1016/j.enggeo.2023.107045

Pirone M, Forte G, Santo A et al (2025) Novel Rainfall Thresholds for Shallow Slip Prediction Based on Field Monitoring: Case Study of the Lattari Mountains, Italy. J. Geotech Geoenvironmental Eng 151:05024016. https://doi.org/10.1061/JGGEFK.GTENG-12797

Qing-zhao Z, Qing P, Ying C et al (2019) Characteristics of landslide-debris flow accumulation in mountainous areas. Heliyon 5:e02463. https://doi.org/10.1016/j.heliyon.2019.e02463

Rehault JP, Moussat E, Fabbri A (1987) Structural evolution of the Tyrrhenian back-arc basin. Mar Geol 74:123–150. https://doi.org/10.1016/0025-3227(87)90010-7

Revellino P, Hungr O, Guadagno FM, Evans SG (2004) Velocity and runout simulation of destructive debris flows and debris avalanches in pyroclastic deposits, Campania region, Italy. Environ Geol 45:295–311. https://doi.org/10.1007/s00254-003-0885-z

Rovida A, Locati M, Camassi R et al (2022) Catalogo Parametrico dei Terremoti Italiani (CPTI15), versione 4.0 [Data set]. Istituto Nazionale di Geofisica e Vulcanologia (INGV). https://doi.org/10.13127/cpti/cpti15.4

Sæmundsson Þ, Morino C, Helgason JK et al (2018) The triggering factors of the Móafellshyrna debris slide in northern Iceland: intense precipitation, earthquake activity and thawing of mountain permafrost. Sci Total Environ 621:1163–1175. https://doi.org/10.1016/j.scitotenv.2017.10.111

Santangelo N, Romano P, Ascione A, Russo Ermolli E (2017) Quaternary evolution of the Southern Apennines coastal plains: a review. Geol Carpath 68:43–56. https://doi.org/10.1515/geoca-2017-0004

Santo A, Massaro L (2024) Landslide monitoring and maintenance plan along infrastructure: the example of the Maratea major rockfall (Southern Italy). Landslides. https://doi.org/10.1007/s10346-024-02409-3

Santo A, Di Crescenzo G, Forte G et al (2018) Flow-type landslides in pyroclastic soils on flysch bedrock in southern Italy: the Bosco de' Preti case study. Landslides 15:63–82. https://doi.org/10.1007/s10346-017-0854-3

Sarkar S, Roy AK, Raha P (2016) Deterministic approach for susceptibility assessment of shallow debris slide in the Darjeeling Himalayas, India. Catena (Amst) 142:36–46. https://doi.org/10.1016/j.catena.2016.02.009

Scardino G, Miglietta MM, Kushabaha A et al (2024) Fingerprinting Mediterranean hurricanes using pre-event thermal drops in sea-water temperature. Sci Rep 14:8014. https://doi.org/10.1038/s41598-024-58335-w

Sidle RC, Swanston DN (1982) Analysis of a small debris slide in coastal Alaska. Can Geotech J 19:167–174. https://doi.org/10.1139/t82-018

Tung BD, Do NH, Thanh NK et al (2021) Geometry and the Mechanism of Landslide Occurrence in a Limestone Area – Case Examples of Landslides in Vietnam and from Europe, China, and Japan –. J Disaster Res 16:646–657. https://doi.org/10.20965/jdr.2021.p0646

Wang G, Sassa K, Fukuoka H (2003) Downslope volume enlargement of a debris slide–debris flow in the 1999 Hiroshima, Japan, rainstorm. Eng Geol 69:309–330. https://doi.org/10.1016/S0013-7952(02)00289-2

Yagi H, Sato G, Higaki D et al (2009) Distribution and characteristics of landslides induced by the Iwate–Miyagi Nairiku Earthquake in 2008 in Tohoku District, Northeast Japan. Landslides 6:335–344. https://doi.org/10.1007/s10346-009-0182-3